

Observing ideal “self-similar” crack growth in experiments

Kaiwen Xia ^{a,*}, Vijaya B. Chalivendra ^b, Ares J. Rosakis ^c

^a *Department of Civil Engineering and Lassonde Institute, University of Toronto, 35 St. George Street, Toronto, Ont., Canada M5S 1A4*

^b *Department of Mechanical Engineering, University of Massachusetts Dartmouth, North Dartmouth, MA 02747, USA*

^c *Graduate Aeronautical Laboratories, California Institute of Technology, Pasadena, CA 91125, USA*

Received 2 January 2006; received in revised form 5 May 2006; accepted 6 May 2006

Available online 7 July 2006

Abstract

We here report on a detailed experimental study whose goal is to investigate spontaneous crack propagation in bonded and intact materials subjected to quasi-static far-field tensile loading. The cracks nucleate from a tiny circular hole and are triggered by an exploding wire. They subsequently propagate under the action of a constant far-field load. Dynamic photoelasticity in conjunction with high speed photography is used to capture the real-time photoelastic fringe patterns (isochromatics) associated with crack propagation. Dynamic stress intensity factors of propagating cracks are determined and the results are successfully compared with Broberg’s classical model of self-similar mode-I crack growth.

© 2006 Elsevier Ltd. All rights reserved.

Keywords: Self-similar crack; Spontaneous dynamic fracture; Broberg’s problem; Dynamic photoelasticity

1. Introduction

Theoretically solvable dynamic fracture problems can be mainly classified into two idealized categories [1,2]. The first category is called “steady-state crack growth”, in which the crack propagates at constant velocity and the mechanical fields are invariant with respect to an observer moving with the crack tip. Two-dimensional Yoffe problem [3] belongs to this category, where a crack of fixed length propagates in a body subjected to uniform far-field tensile loading. The second category of problems is called “self-similar crack growth” [2], in which two crack tips move at constant velocity symmetrically from a zero initial length and mechanical fields are invariant with respect to an observer moving steadily away from the crack nucleation point. The original two-dimensional problem studied by Broberg [4] which will be referred to here as the “Broberg’s problem” belongs to this category. Based on same assumptions of Broberg problem, Burrige and Willis [5] investigated the self-similar problem of the expanding elliptical crack in an anisotropic solid. Willis [6] also developed elastodynamic formulation of several self-similar mixed boundary-value problems. Recently,

* Corresponding author. Tel.: +1 416 946 5712; fax: +1 416 978 6813.

E-mail address: Kaiwen.Xia@utoronto.ca (K. Xia).

Broberg [7] reported that the observed slow terminal crack velocities of a mode-I crack can be understood within the framework of the self-similar crack theory by invoking the similarity of the crack process zone size.

Experimental studies on dynamic crack propagation reported so far have used both stress wave loading to initiate and grow a crack, and statically loaded specimen that dynamically growing cracks are allowed to grow from a blunted notch [8]. Ravichandar and Knauss [9] studied a mode-I crack propagation problem using a transient crack face loading configuration. Another example of this was discussed by Ravichandran and Clifton [10], who studied mode-I crack propagation in a pre-cracked homogeneous material subjected to plane wave loading. Using the same idea as Ravichandar and Knauss [9], Washabaugh and Knauss [11] investigated the limiting crack speed of mode-I cracks propagating along an interfaces between weakly bonded plates. Finally Rosakis and his co-workers [12–16] have studied crack propagation along bonded (coherent) interfaces between similar or dissimilar materials using dynamic shear loading induced by projectile impact. For dissimilar material systems, they found that the shear crack could propagate at a speed faster than the dilatational wave speed of the slower wave speed constituent material often becoming “supersonic” with respect to one side. For similar material systems, however the shear cracks propagating along interfaces could grow at a speed faster than the shear wave speed of the material, and they often approached the longitudinal wave speed for large enough loading [14]. Such cracks are called “supershear” cracks.

Beebe [17] tried to investigate self-similar crack growth by using central crack specimen geometry with far-field tensile loading. There are two major limitations in this work: (a) There are singular stress fields around the crack tips instead of uniform stress field that required by the Broberg’s problem; (b) No complete comparison of experimental results with Broberg theory was made. Spontaneous crack propagation processes require quasi-static pre-existing loading and crack growth from a zero initial length. There are a few important reasons to motivate the experimental study of spontaneous crack growth for the case of mode-I loading conditions as initially proposed by Broberg [1,4]. First of all, there are many practical examples involving spontaneous fracture and catastrophic failure of civil and defense structures. Such examples involve defects of initial sizes that are often negligible compared to a whole structure which is subjected to quasi-static tensile loading. Secondly, most of the modern engineering materials such as fiber reinforced composites, graded and bonded materials and structures, have interfaces which are either coherent (have intrinsic strength and toughness) or incoherent (are either damaged or have frictional strength). Since interfaces are usually weaker than the constituent materials, their spontaneous interface failure is the active failure mechanism in such solids [18]. Indeed any defects in such interfaces can ultimately serve as sites of catastrophic failure nucleation during the service life of the structure.

Motivated by above issues, a novel experimental technique is designed and developed to induce spontaneous crack growth along interfaces separating bonded plates. In order to simulate spontaneous dynamic fracture, an exploding wire technique is used to nucleate fracture from a very small hole in the specimen. Far-field tensile loading is used to drive the subsequent dynamic crack propagation following crack nucleation. Dynamic photoelasticity in conjunction with high-speed photography is used to capture real-time isochromatic fringe patterns associated with the entire event. These fringe patterns are analyzed to obtain crack tip position and crack propagation velocities. A nonlinear least-square method is used to determine dynamic mode-I stress intensity factor histories from the fringes. Since the experiments reveal constant crack tip velocities for each far-field level of stress, the spontaneous crack growth configuration studied also corresponds to the ideal conditions of “self-similarity” described above. Consequently, the stress intensity factor histories are used to compare with the classical, self-similar, crack growth model originally proposed by Broberg [4].

2. Experimental details

Two different birefringent materials, Homalite-100 and polycarbonate are used in this study. The material properties are listed in Table 1. The wave speeds are measured using ultrasonics while the rest of the properties are taken from the literature [19]. Since polycarbonate material is tough and it needs much higher loads to nucleate and grow unstable cracks in intact polycarbonate sheets, Homalite-100 is used to study crack propagation in intact plates. The dimensions of the specimen are 150 mm × 150 mm. For the intact Homalite-100 specimens, a small through thickness hole of 0.1 mm in diameter is drilled at the center of the specimen to hold an exploding wire. The size of the exploding wire is slightly smaller than that of the hole. In case of bonded

Table 1
Optical and mechanical properties of photoelastic materials used in this study

| Material | Homalite-100 | Polycarbonate |
|--|--------------|---------------|
| Young's modulus E (MPa) | 3860 | 2480 |
| Poisson's ratio ν | 0.35 | 0.38 |
| Stress fringe value f_σ (kN/m) | 23.6 | 7.0 |
| Plane stress P wave speed C_P (km/s) | 2.104 | 1.724 |
| S wave speed C_S (km/s) | 1.200 | 0.960 |
| Density ρ (kg/m ³) | 1230 | 1192 |

polycarbonate specimen, a small groove of 0.1 mm in width and depth is made on the bonding interface of one of the two 150 mm \times 75 mm sheet along the thickness direction. Then the two polycarbonate sheets are glued together with a HARDMAN five minute epoxy adhesive with the exploding wire sitting in the groove.

Fig. 1(a) shows the experimental setup used in this study. It consists of laser light source, a set of circular polarizer sheets, a high speed camera, and an explosion box. A collimated beam is used to illuminate the specimen, which is sandwiched between two circular polarizer sheets. The explosion box provides the electric energy to explode the wire, which is the critical part of the design of this spontaneous fracture problem. The details of the explosion box were duly discussed in Refs. [20,21]. The electronic explosion results in an expanding plasma wave. For the bonded specimen, this explosion creates a small crack along the interface if the toughness of the adhesive is much weaker than that of the material. Under large enough static far-field loading, this initial small crack is unstable and will propagate. For the intact material, the explosion creates micro-cracks on the wall of the small hole in random radial directions. If the specimen is also subjected to far-field tensile loading, only the micro-cracks perpendicular to the loading axis will propagate dynamically. Upon

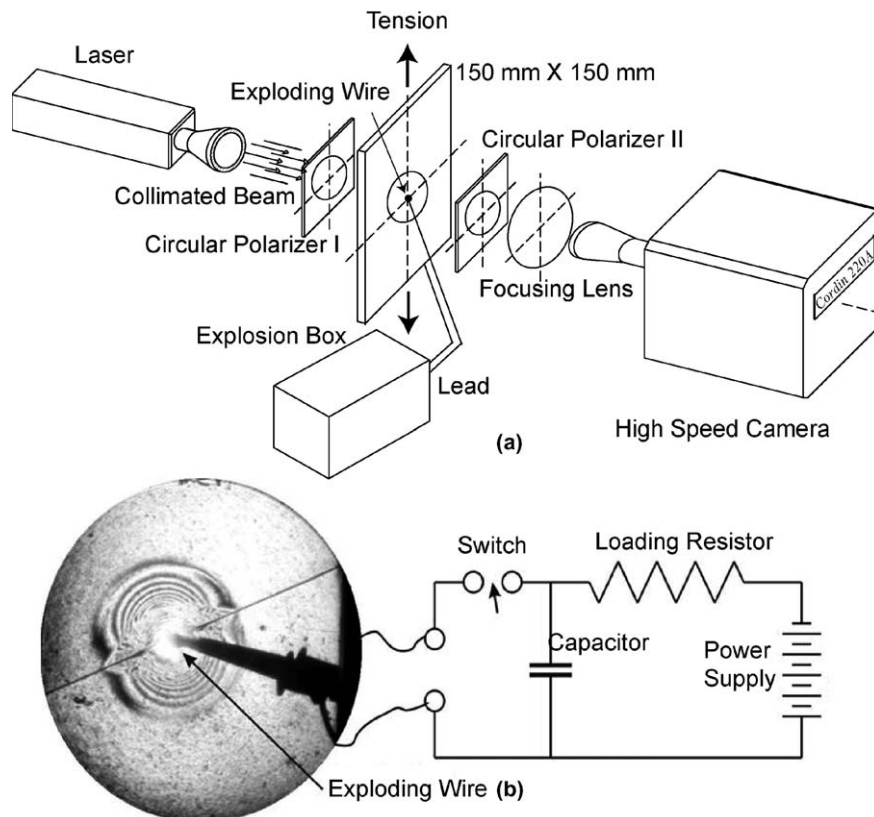


Fig. 1. Experimental setup (a) with exploding wire circuit (b).

sending the high electric energy to the exploding wire, the explosion box also sends a triggering signal to the high speed camera. We used Cordin 200 ultra high speed camera in our study. The camera system, which is digital, is able to capture the images at a framing rate of 100 million frames/s with exposure times as low as 10 ns. In this study, the high speed camera is operated at a much slower speed, around 0.2–0.4 million frames/s. Fig. 1(b) shows the photograph of isochromatic fringe pattern generated by an explosion at an incoherent interface between two plates. The existence of a dilatational wave front, a shear wave front and a head wave can be clearly seen from the figure. The head wave intersects with the interface and is tangent to the shear wave front.

3. Experimental results and discussion

A set of experiments is performed whose purpose is to observe spontaneous crack propagation at different crack tip velocities. In order to achieve this, two specimen configurations are considered as described above. For lower crack propagation velocities, intact Homalite-100 plates are used. For higher propagation velocities, weakly bonded polycarbonate plates are used. The magnitude of the far-field tensile stress is also varied to obtain different velocity levels. Typical values of far-field stresses used range from 4 MPa to 10 MPa.

3.1. Isochromatics of propagating cracks

Typical isochromatic fringe patterns for two different cases (intact Homalite-100 and bonded polycarbonate specimens) are shown in Fig. 2, and in all cases upon nucleation, the crack propagates symmetrically in both directions from the center of the specimen. In order to simulate the theoretical assumption of crack

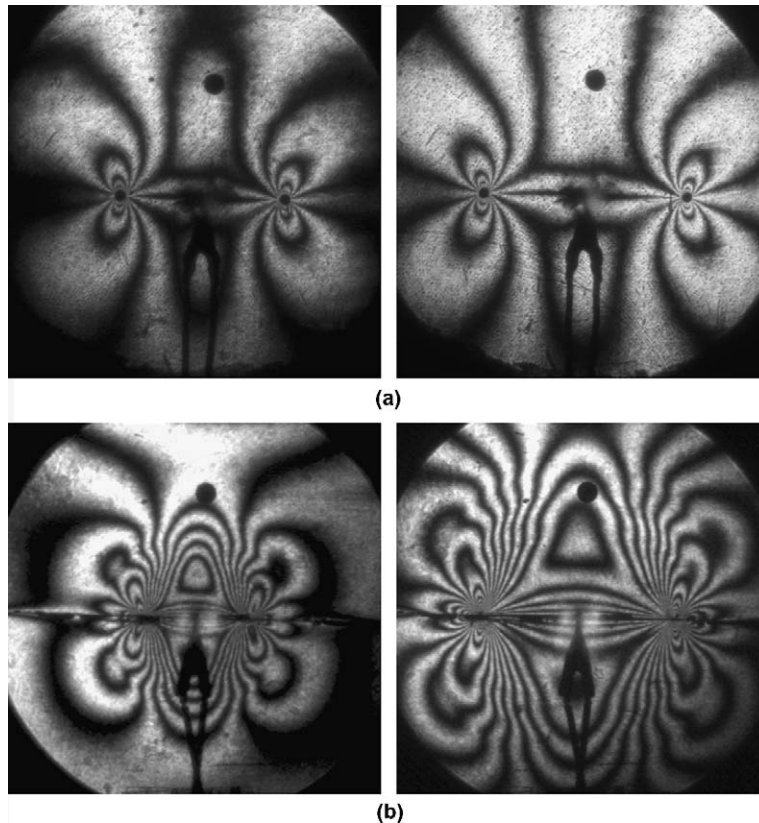


Fig. 2. Isochromatic fringes of propagating crack in (a) Homalite-100 intact material and (b) layered polycarbonate material at different time instances. The black dot in the pictures is a 6.25 mm scale.

growth in an infinite domain, the crack propagation process is recorded at times prior to the arrival of the reflected waves from the specimen boundaries. Accurate crack tip positions for the propagating cracks can be identified by the shadow spots corresponding to the traveling stress singularity. These are clearly visible in the figure. In Fig. 2(a), the fringes are shown for a Homalite-100 specimen. The isochromatic fringes for weakly bonded polycarbonate plates are shown in Fig. 2(b). It can be observed from Fig. 2 that the size and number of isochromatic fringes increase as the crack length increases around both crack tips. These fringes clearly correspond to textbook equi-bilateral mode-I crack propagation since they are perfectly symmetric with respect to both the crack line and the nucleation point.

3.2. Crack tip position and crack velocity

The crack tip positions associated with the propagating crack tips are obtained from extrapolating to the center of the shadow spot surrounding each tip. The crack tip position as a function of the time for two cases, intact Homalite-100 and bonded polycarbonate plates is shown in Fig. 3(a) and (b), respectively. It can be seen from these figures that the crack tip velocities are constant within the error of the measurement. The propagation velocity for Homalite-100 specimen in Fig. 3(a) is approximately 395 m/s, for both crack tips, while the propagation velocity for bonded specimen in Fig. 3(b) is ≈ 650 m/s. It is important to mention here that the crack tips accelerate almost instantaneously to a constant velocity upon nucleation of the dynamic fracture event. As a consequence, our experiments satisfy one of the basic requirements (assumptions) for “self-similar” crack growth. The other requirement has already been met because the dynamic cracks are nucleated from a very small hole, which is essentially infinitesimal in size as compared to any length scale of the plate specimen.

3.3. Dynamic stress intensity factors

Asymptotic crack tip stress fields for steady-state crack propagation [22] combined with the stress optic law as given below in Eq. (1) define the isochromatics at a given point around the crack tip as follows:

$$\tau_{\max} = \frac{\sigma_1 - \sigma_2}{2} = \frac{Nf_{\sigma}}{2h} \quad (1)$$

In the above equation, τ_{\max} is the maximum shear stress, σ_1 and σ_2 are maximum and minimum principal stresses respectively, N is the fringe order, f_{σ} is material fringe constant, and h is thickness of the specimen. The fringe orders of selected set of points (between 75 and 100 points) are obtained from one inch diameter region around the crack tip. The dynamic mode-I stress intensity factor, K_I^d , values are determined from these points using eight terms in the asymptotic expansion and a non-linear least-squares method in conjunction with the Newton–Raphson technique [19]. In order to have a confidence over extracted dynamic mode-I stress intensity factor values, the determined coefficients of eight terms are used in regenerating synthetic isochromatic contours and it is identified that the fringe orders of chosen data points matched well with regenerated

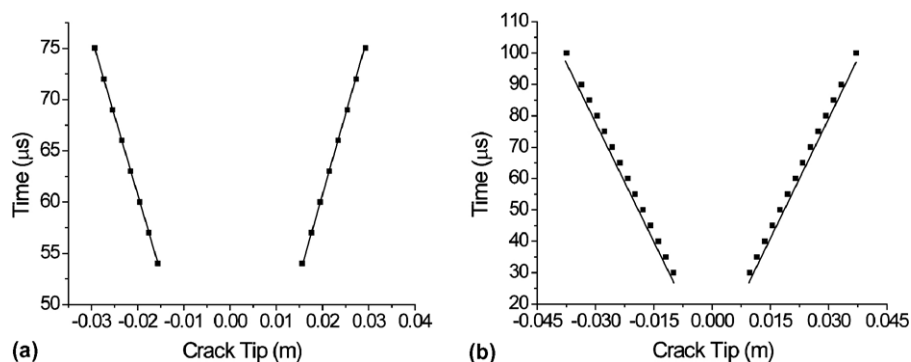


Fig. 3. Crack tip position as a function of time in (a) Homalite-100 intact material and in (b) weakly bonded polycarbonate material.

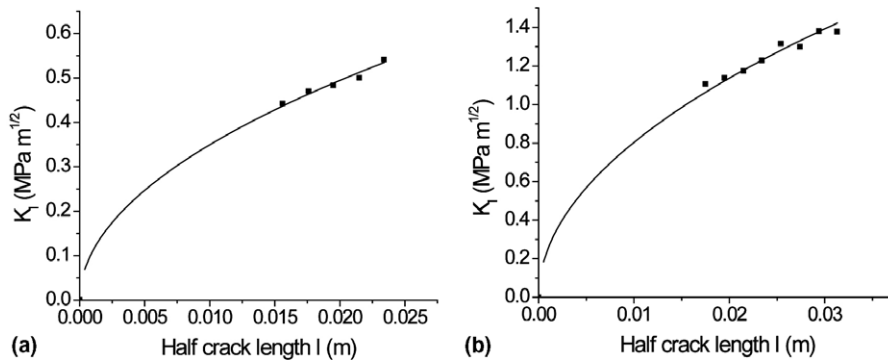


Fig. 4. Dynamic stress intensity factor history of propagating crack in (a) intact Homalite-100 and in (b) weakly bonded polycarbonate sheets. The solids lines are fittings using Eq. (4) as discussed in Section 4.2.

contours. The variation of dynamic stress intensity factor as a function of crack tip position for the right-hand crack tip for the two cases discussed in the previous section (3.2) is shown in Fig. 4. Fig. 4(a) shows the variation of K_I^d as function of half crack length (l) for the Homalite-100 specimen. The variation of K_I^d for the weakly bonded polycarbonate plates is shown in Fig. 4(b). It can be seen from both figures that the experimentally measured K_I^d varies as $l^{1/2}$.

4. Comparison of experimental results with Broberg’s problem

4.1. Broberg’s theoretical results

Broberg [4] solved a self-similar crack propagation problem which is very closely approximated by our experimental setup as described above. The time history of the dynamic stress intensity factor $K_I^d(t, v)$ is related with the following expression:

$$\frac{K_I^d(t, v)}{K_{I0}} = - \frac{I(b/h)R(h)}{b^2 h \sqrt{h^2 - a^2}} = c \tag{2}$$

where $K_{I0} = \sigma_\infty \sqrt{\pi l/2}$, σ_∞ is the far-field loading, v is the crack velocity, a is the inverse of dilatational wave speed C_P , b is the inverse of shear wave speed C_S , h is the inverse of the crack speed v , and $R(\xi) = (b^2 - 2\xi^2)^2 + 4\xi^2 \sqrt{a^2 - \xi^2} \sqrt{b^2 - \xi^2}$ is the Rayleigh function. The function $I(b/h)$ can be expressed as:

$$I(b/h) = \frac{b^2}{h} \int_0^\infty \frac{R(i\eta)}{(h^2 + \eta^2)^{3/2} \sqrt{a^2 + \eta^2}} d\eta \tag{3}$$

For given crack velocity, the right-hand side of Eq. (2) is a constant c , which can be evaluated using Eq. (3). The values of $c = K_I^d(t, v)/K_{I0}$ as a function of velocity for both Homalite-100 and polycarbonate materials are shown as solid lines in Fig. 5. The theoretical curves for both materials fall on top of each other because they depend on the Poisson’s ratio of the materials and their difference is very small.

4.2. Experimental determination of c and the comparison with the Broberg’s model

By using the expression $K_{I0} = \sigma_\infty \sqrt{\pi l/2}$, Eq. (2) now reduces to

$$K_I(t, v) = c \sigma_\infty (\sqrt{\pi/2}) l^{1/2} = c_1 l^{1/2} \tag{4}$$

where $c_1 = c \sigma_\infty \sqrt{\pi/2}$. The new constant c_1 can be estimated by fitting the experimentally obtained K_I^d versus half crack length (l) record to the square root of half crack length (l) as shown in Fig. 4. Then by using the relation $c_1 = c \sigma_\infty \sqrt{\pi/2}$, the ratio $c = K_I^d(t, v)/K_{I0}$ can also be estimated from the experiments. Two experiments of intact Homalite-100 plates and three experiments featuring bonded polycarbonate plates are

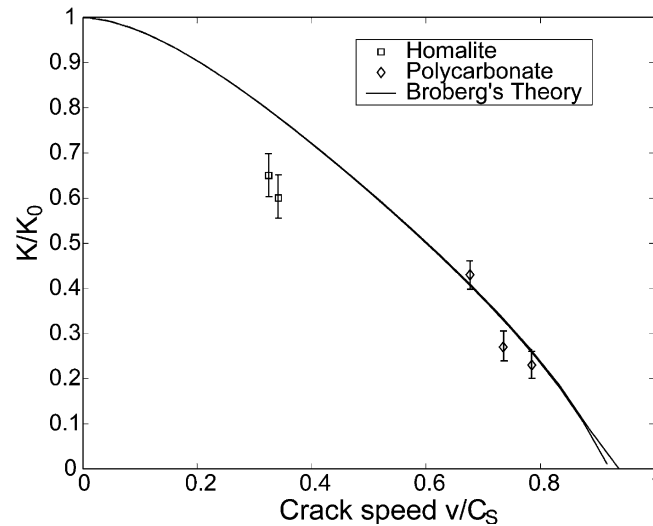


Fig. 5. Comparison of experiment with the Broberg theory.

Table 2
List of parameters of the experiments

| Test # | 1 | 2 | 3 | 4 | 5 |
|-------------------------|--------|--------|--------|--------|--------|
| Sample type | Bonded | Bonded | Bonded | Intact | Intact |
| σ_{∞} (MPa) | 8.8 | 8.0 | 4.5 | 9.9 | 7.5 |
| V (m/s) | 754 | 706 | 650 | 410 | 390 |

conducted to obtain dynamic stress intensity factor histories as functions of crack length. The experimentally determined values of c for all these five experiments are plotted along with Broberg's model in Fig. 5. The results indicate that there exists a considerable amount of agreement between the experimental results and Broberg's model. However, there is a slight difference between the theory and the experimental results in the case of intact Homalite-100 specimens. The reason for this difference may be attributed to the fact that the apparent far-field load applied to propagate the central (horizontal) crack is less than the applied far-field load. As mentioned previously in Section 2, there exist several radial micro-cracks surrounding the explosion location at the center of the specimen created by the explosion. The applied far-field load might have been reduced due to the additional release waves from the crack faces of these micro-cracks around the explosion hole, which also propagate a very small distance around the explosion area while the central crack is growing. This discrepancy might be diminished if we have a better way to initiate the crack. Parameters of all five experiments given in Fig. 5 are listed in Table 2.

5. Conclusions

An experiment setup has been designed to induce "spontaneous" mode-I fracture propagation. The crack velocities are found to be constant within each experiment. However the magnitude of these velocities varies with the level of far-field loading. The experimental configuration and the naturally resulting constant velocities correspond to the ideal case of "self-similar" crack growth. Indeed, the experiments approximate closely the two most important requirements for assuring "self-similar" crack growth as assumed by Broberg in his classical model. These are the initiation (nucleation) of crack growth from a zero crack length and its growth under a constant velocity. The experimental records of photoelastic fringes are analyzed to determine the dynamic stress intensity factor values of crack propagation. These results are successfully compared with the theoretical predictions by Broberg. It can be concluded from this study that self-similarity of spontaneous crack growth as assumed by Broberg is a surprisingly accurate representation of physical reality.

Acknowledgements

The authors would like to acknowledge the support of the Office of Naval Research (ONR) through grant number N00014-03-1-0435 (Dr. Y.D.S. Rajapakse, project monitor). Helpful discussions with Prof. G. Ravichandran from Caltech, with Prof. A. Shukla from University of Rhode Island, and with Prof. L.B. Freund at Brown University are also acknowledged.

References

- [1] Broberg KB. Cracks and fracture. San Diego: Academic Press; 1999.
- [2] Freund LB. Dynamic fracture mechanics. Cambridge, New York: Cambridge University Press; 1990.
- [3] Yoffe EH. The moving Griffith crack. *Philos Mag* 1951;42(330):739–50.
- [4] Broberg KB. The propagation of a brittle crack. *Arkiv Fysik* 1960;18(2):159–92.
- [5] Burridge R, Willis JR. Self-similar problem of expanding elliptical crack in an anisotropic solid. *Proc of the Cambridge Philos Soc Math Phys Sci* 1969;66:443–68.
- [6] Willis JR. Self-similar problems in elastodynamics. *Philos Trans Royal Soc London Ser A – Math Phys Engng Sci* 1973;274(1240):435–91.
- [7] Broberg KB. Constant velocity crack propagation – dependence on remote load. *Int J Solids Struct* 2002;39(26):6403–10.
- [8] Shukla A, Nigam H. A note on the stress intensity factor and crack velocity relationship for Homalite-100. *Engng Fract Mech* 1986;25(1):91–102.
- [9] Ravichandar K, Knauss WG. An experimental investigation into dynamic fracture. I. Crack initiation and arrest. *Int J Fract* 1984;25(4):247–62.
- [10] Ravichandran G, Clifton RJ. Dynamic fracture under plane-wave loading. *Int J Fract* 1989;40(3):157–201.
- [11] Washabaugh PD, Knauss WG. A reconciliation of dynamic crack velocity and Rayleigh-wave speed in isotropic brittle solids. *Int J Fract* 1994;65(2):97–114.
- [12] Lambros J, Rosakis AJ. Development of a dynamic decohesion criterion for subsonic fracture of the interface between two dissimilar materials. *Proc Royal Soc London Ser A – Math Phys Engng Sci* 1995;451(1943):711–36.
- [13] Lambros J, Rosakis AJ. Dynamic decohesion of bimetals – Experimental-observations and failure criteria. *Int J Solids Struct* 1995;32(17–18):2677–702.
- [14] Rosakis AJ, Samudrala O, Coker D. Cracks faster than the shear wave speed. *Science* 1999;284(5418):1337–40.
- [15] Rosakis AJ, Samudrala O, Coker D. Intersonic shear crack growth along weak planes. *Mater Res Innov* 2000;3(4):236–43.
- [16] Coker D, Rosakis AJ, Needleman A. Dynamic crack growth along a polymer composite–Homalite interface. *J Mech Phys Solids* 2003;51(3):425–60.
- [17] Beebe WM. An experimental investigation of dynamic crack propagation in plastic and metals. In: AFML-TR-66-249, Air Force Materials Laboratory Technical Report. 1966.
- [18] Rosakis AJ. Intersonic shear cracks and fault ruptures. *Adv Phys* 2002;51(4):1189–257.
- [19] Dally JW, Riley WF. Experimental stress analysis. 3rd ed. New York: McGraw-Hill Inc; 1991.
- [20] Xia KW, Rosakis AJ, Kanamori H. Laboratory earthquakes: The sub-Rayleigh-to-supershear rupture transition. *Science* 2004;303(5665):1859–61.
- [21] Xia KW et al. Laboratory earthquakes along inhomogeneous faults: Directionality and supershear. *Science* 2005;308(5722):681–4.
- [22] Liu C, Rosakis AJ. On the higher-order asymptotic analysis of a nonuniformly propagating dynamic crack along an arbitrary path. *J Elasticity* 1994;35(1–3):27–60.